Stochastic modeling of climatic variability in dendrochronology

Daniel Lavallée[1] and Hugo Beltrami[2]

Received 14 April 2004; revised 14 May 2004; accepted 13 July 2004; published 6 August 2004.

[1] Climatic variability can be characterized by invariant quantities arising from the analysis of scaling properties of paleoclimatic records. In this paper we discuss a stochastic model that reproduces the variability and the long-range correlation observed in dendrochronological time series. We have found that non-Gaussian distributions are better suited to describe the climatic variability embedded in these data. Our results indicate that Gaussian distribution fails to capture the large fluctuation —extreme events— that characterized climatic variability in these time series. This might have applications on the study of extreme weather events on future climate scenarios. *INDEX TERMS:* 1620 Global Change: Climate dynamics (3309); 1610 Global Change: Atmosphere (0315, 0325); 1699 Global Change: General or miscellaneous; 3210 Mathematical Geophysics: Modeling. **Citation:** Lavallée, D., and H. Beltrami (2004), Stochastic modeling of climatic variability in dendrochronology, *Geophys. Res. Lett.*, *31*, L15202, doi:10.1029/2004GL020263.

1. Introduction

[2] Most records of climate change show increase warming since the industrial revolution [*Houghton et al.*, 2001]. Furthermore, it has also been shown that at the climate system scale, that oceans, cryosphere, atmosphere and continental areas have absorbed heat in the last 50 years on the order of 182.0, 8.1, 6.6 and 7.1 (10^{21}) Joules respectively [*Levitus et al.*, 2001; *Beltrami et al.*, 2002; *Beltrami*, 2002]. The question is whether the additional energy available in the climate system coupled to anthropogenic changes in the environmental conditions at the Earth's surface, for example, due to land use changes, might lead to a more vigorous atmospheric circulation and thus our climate might experience an increased number of extreme weather events. Such a change has serious implications for society and has attracted much attention from policy makers and the general public. In order to assess the number, magnitude, and character of extreme weather events in a future warmer climate, models of the climate system have been used to study the statistics of climate model outputs (e.g., V. V. Kharin and F. W. Zwiers, Estimating extremes in transient climate change simulations, submitted to *Journal of Climate*, 2004; G. C. Hegerl et al., Detectability of anthropogenic changes in temperature and precipitation extremes, submitted to *Journal of Climate*, 2004). To assess whether the frequency of extreme weather events will increase in a warmer future Earth's climate, it is also important to understand and model the frequency of occurrence of extreme weather events in the past. One of the records with highest resolution of past environmental conditions, in temperate latitudes, are dendrochronological data. Tree ring records have been routinely used to reconstruct past climatic changes [e.g., *Cook and Briffa*, 1990; *Stahle et al.*, 2000; *Cook et al.*, 2000; *Esper et al.*, 2001, 2002]. Recent multiproxy reconstructions of the past climate of the northern hemisphere made important use of dendrochronological records [e.g., *Mann et al.*, 1999, see chapter 2 in *Houghton et al.*, 2001].

[3] In this letter, we examine four long dendrochronological records from the western United States selected from the International Tree Ring Databank (ITRDB) (see Table 1). The tree ring data were selected for this study because of their large temporal coverage and their likelihood to be moisture or temperature sensitive.

[4] One important feature of the dendrochronological data is its complex behavior (see Figure 1). Note that the time evolution of the signal is erratic showing no apparent regularity or cyclic pattern. In this letter, we propose to decipher the "complexity" embedded in the dendrochronological records in term of its statistical properties. For this purpose, we present a stochastic model that reproduce the probability law and correlation function (or power spectrum) observed in the dendrochronological records.

2. Formulation of the Stochastic Model

[5] To analyze the complex behavior of the dendrochronological time series, a typical procedure consists in performing a Fourier analysis of the time series. The power spectrum of one time series is illustrated in Figure 2. The spectrum shows that there are no dominating frequencies, and that these signals cannot be reduced to—or understood as— a combination of several periodical functions. Figure 2, shows that all the frequencies contribute to the signals but also that the weight of the frequencies follows —on average— a trend given by a decaying power law. The values of the scaling exponents ν are reported in Table 2.

[6] The behavior reported in Figures 2 is typical of colored noises. According to this, a stochastic model can capture and reproduce some of the main features characterizing the dendrochronological time series. The stochastic model proposed here consists of a convolution in the frequency space between the Fourier transform of random variables (white noise) X and some function with a power law dependence $\omega^{-\nu/2}$. The scaling exponent ν measures the departure from the non-correlated random variable (white noise with $\nu = 0$), ω is the angular frequency. This stochastic process is similar to a fractional Brownian motion that reduces to a random walk in its simplest manifestation — with $\nu = 2$ and X a Gaussian random variable [see *Peitgen and Saupe*, 1988; *Falconer*, 1990]. In this study, the

[1]Institute for Crustal Studies, University of California, Santa Barbara, USA.
[2]Environmental Earth Sciences Laboratory, St. Francis Xavier University, Antigonish, Nova Scotia, Canada.

0094-8276/04/2004GL020263$05.00

Table 1. The Dendrochronological Data Used in This Study

Tree-Ring	Location	Species	Years
nv500	38°-57′N–114°-13′W	Bristlecon Pine	1–1967
nv512	40°-14′N–115°-32′W	Bristlecon Pine	320–1985
nv514	40°-33′N–114°-49′W	Bristlecon Pine	302–1985
ut508	39°-25′N–111°-04′W	Bristlecon Pine	286–1985

parameter ν and the probability law that governs the distribution of the random variables are unspecified. They are determined through a statistical analysis of the data. The stochastic model Y_t is given by the following relationship:

$$Y_t \propto \sum_{s=1}^{N} \omega^{-\nu/2} F_\omega[X_t] \exp[2\pi i(t-1)(s-1)/N], \quad (1)$$

for a set of random variables X_t distributed over a one–dimensional lattice of length N, where t is the integer time variable on the one-dimensional lattice. The sum in equation (1) goes from 1 to N; s is related to ω by $\omega = 2\pi(s - 1)$ and corresponds to a discrete frequency with integer values; $F_\omega[X_t]$ is the discrete Fourier transform of the random variables. According to this, the power spectrum $P(k)$ associated to Y_t will be given by the following relation:

$$P(\omega) = |F_\omega[Y_t]|^2 \propto \omega^{-\nu}. \quad (2)$$

This equation can be used to compute the values of the parameter ν associated to Y_t. Using this scaling exponent ν, the underlying random variables X_t associated to a stochastic model Y_t can be computed by using the following relationship:

$$X_t \propto F_t^{-1}\left[F_\omega[Y_t] \times \omega^{\nu/2}\right], \quad (3)$$

where F_t^{-1} is the Fourier inverse. The statistical properties of the stochastic model are completely specified when the probability law governing X_t are identified. The probability law controls the variability of the stochastic model while ν constraints its long-range correlation (see *Lavallée and Archuleta* [2003] for another application of this stochastic model).

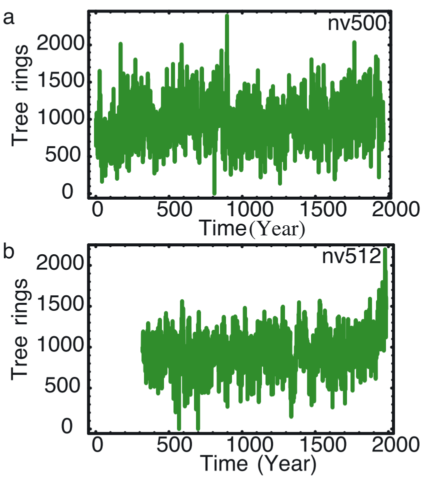

Figure 1. The typical behavior of the time evolution of the tree ring indices is illustrated: (a) nv500 and (b) nv512. The time interval is one year on each sample.

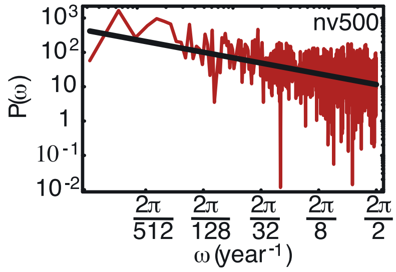

Figure 2. For the signal illustrated in Figure 1a, the power spectrum $P(\omega)$ has been computed. The power spectrum $P(\omega)$ (red) and the best straight line (black) that fits the log-log curve is reported for this signal. These results suggest that the scaling behavior is observed for time scale length ranging from 2 to 512 years. The scaling exponent is given in Table 2.

3. Stochastic Model for Dendrochronological Time Series

[7] In this letter, we assume that a dendrochronological time series can be approximated by a stochastic model Y_t described above. Using relation (2), the scaling exponent ν of each time series has been computed. Then, using ν and equation (3), the underlying random variables X_t associated to each time series are estimated. The number of random variables in the time series varies between 1666 (nv512) to 1967 (nv500). These numbers are large enough to perform the ensuing statistical analysis. For each tree ring sample, the probability density function (PDF) associated with X_t is thus estimated.

[8] We then proceed to determine the probability law that will provide the best fit to the estimated PDF of X_t. Three candidates are considered: the Gauss law, the Cauchy law and the more general Lévy law [*Uchaikin and Zolotarev*, 1999]. The Lévy law is characterized by four parameters α, β, γ and μ. The parameter α, with $0 < \alpha \leq 2$, controls the rate of falloff of the tails of the PDF. The larger the value of α, the less likely it is to find a random variable far away from the central location. The case $\alpha = 2$ corresponds to the Gaussian law while $\alpha = 1$ (with $\beta = 0$) corresponds to the Cauchy law. The parameter β, with $-1 \leq \beta \leq 1$, controls the departure from symmetry of the PDF curve. When $\beta = 0$, the PDF is symmetric and centered about μ. The parameter γ, $\gamma > 0$, is mainly responsible for the PDF width whereas μ is the location or shift parameter of the PDF.

[9] For each tree ring sample, we have computed the probability law parameters that minimize the following expression:

$$\sum_t |PDF(X_t) - p_{th}(X_t)| \quad (4)$$

where $p_{th}(X)$ corresponds the theoretical values of the PDF associated to either the Gauss, Cauchy or Lévy law computed for X [see *Grigoriu*, 1995]. The PDF of X and the PDF curves corresponding to the best-fitting Gaussian, Cauchy and Lévy law are illustrated in Figures 3, 4 and 5.

Table 2. Parameters of the Stochastic Models for the Four Tree Ring Indices: nv500, nv512, nv514 and ut508[a]

		Gauss Law		Cauchy Law		Lévy Law			
Samples	Scaling Exponent ν	μ	σ	γ	μ	α	β	γ	μ
nv500	0.52	−3.59	153.	117.	−8.67	1.72	0.22	3211	9.99
nv512	0.63	15.23	99.1	76.8	16.43	1.62	−0.49	953	−5.73
nv514	0.7	−4.04	94.7	71.7	−6.42	1.76	0.28	1567	5.03
ut508	0.56	17.31	147.	110.	22.12	1.74	−1.0	3131	−21.1

[a]The parameter ν is the scaling exponent of the power spectrum (see Figure 2). The parameters of the Gauss law (μ and σ), the Cauchy law (γ and μ) and the Lévy law (α, β, γ and μ) that best fit the four PDF(X) are given (see Figures 3, 4 and 5).

For each tree ring sample, the parameters of the best-fitting Gaussian, Cauchy and Lévy laws are reported in Table 2. For each sample used in this study, the Lévy law provided the best fit to the PDF. For instance, the minimum values of the objective function given in equation (4) computed for the Cauchy, Gauss and Lévy laws are respectively: 0.0049, 0.0023 and 0.0013 for nv512. Note also that if we perform the same analysis over a comparable number of generated Cauchy, Gauss and Lévy random variables characterized by parameter values similar to those reported in Table 2, we will able to recover the parameters values with enough accuracy to distinguish the three laws. In Figures 4 and 5, comparison of the tails of the PDF to the tail of the best fitting Gaussian and Cauchy curves confirms that the a Lévy law with $1 < \alpha < 2$ provides a better fit.

[10] Variation in the model parameters from one sample to another may suggest a spatial dependence. However, the variation may also reflect, at least partially, the presence of additional noisy effects and other uncertainties in the data. Further investigations are needed to reach a definitive conclusion.

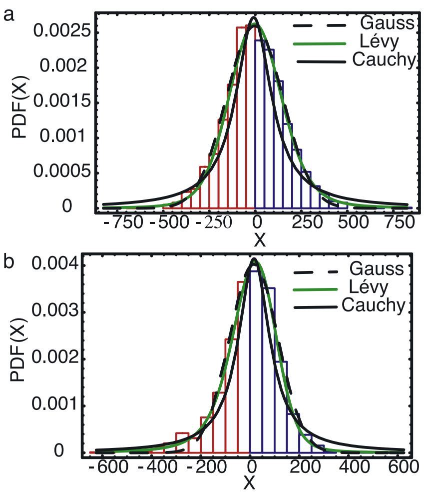

Figure 3. The (discrete) probability density function PDF (red and blue dots and bars) associated to the filtered signal is illustrated: (a) nv500 and (b) nv512. The left side of the PDF ($X < 0$) is colored in red while the right ($X > 0$) side is in blue. The magnitude of the random variables is given by X. The width of the bar corresponds to the increment used to estimate the PDF is equaled to 50. The curves of three probability laws that best fit the PDF are illustrated: the Cauchy law (black curve), the Gaussian law (dashed curve) and the Lévy law (green curve). The parameters of the Gaussian, Cauchy and Lévy law are reported in Table 2.

[11] For the four samples under studies, the value of the Lévy index α doesn't vary very much from one sample to another. This suggests that the value of α may be universal or independent of the tree location. Furthermore, the parameter α, controls the decrease of the PDF tail. That is the occurrence of large fluctuations or extreme events in the data. For instance, using the parameters given in Table 2, one can easily compute, for a given period of time, the number of time that X that exceed a given threshold value. For dendrochronological data, these large fluctuations could be understood as abrupt climatic change. For the four samples, our results suggest that the probability to observe such events deccreases almost at the same rate. The parameters β and γ reported in Table 2 indicate significant variation in the values estimated from one sample to another. (It should be noted that the values estimated for the parameter γ will depend on the definition adopted for the inverse Fourier transform used in equation (3). However, the values of α and β are not affected by this definition.) Note that for $s = 1$, $\omega = 0$ in the convolution given by equation (3). This implies that the average value of the random variables estimated with equation (3) will be zero. This will affect the values taken by the location parameter μ and suggest that not too much importance should be granted to the values taken by this parameter.

[12] Finally note that the values taken by the parameters of the Levy law provide valuable information about the variability of the time series. The parameter γ controls the amplitude of the variability. This is why departures (or

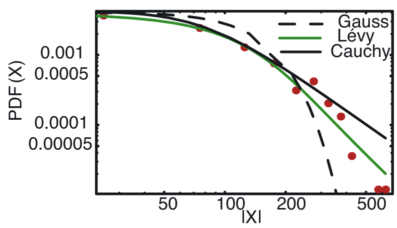

Figure 4. On a log-log plot, the left tail of the (discrete) probability density function PDF (red dot) associated to the filtered signal is illustrated for nv512. The curves of three probability law that best fit the PDF are illustrated: the Cauchy law (black curve), the Gaussian law (dashed curve) and the Lévy law (green curve). Tails that decay according to power laws characterize the Lévy and Cauchy probability density functions. Such behavior is best illustrated on a log-log plot. The misfit of the Gaussian probability density function is more obvious in these plots (see also Figure 5). In particular, note that according to the Gaussian law, the large events have almost a zero probability of being observed.

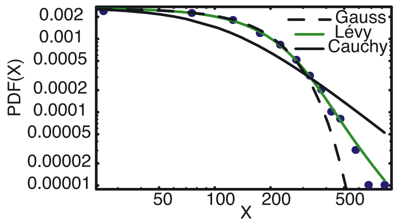

Figure 5. Same as for Figure 4, but for nv500 and for the right tail of the (discrete) PDF (blue dot).

fluctuations) from the average trend of the time series are larger in Figure 1a than in Figure 1b as suggested by the estimated γ reported in Table 2. For a positive β, the tail of the PDF will decay more rapidly for negative values indicating that positive values are more likely to be observed. This implies for a time series approximated by a stochastic model given by equation (1) that positive jumps from the average values are more likely to be observed. The converse applies to negative value of β [see *Uchaikin and Zolotarev*, 1999, Figure 4.13]. Although it is not necessary easy to capture on a plot the isolated effect due to one parameter of the Lévy law when comparing two signal characterized by four different parameter values, comparison of Figures 1a to 1b illustrates well the consequences due to a variation in the polarity of the parameter β.

4. Conclusion

[13] In this paper, we investigated the variability of four dendrochronological records. We have shown that a stochastic model — based on Lévy law— is best suited to reproduces the main features of the climatic variability embedded in dendrochronological time series, including the presence of large fluctuations. (For a comparison between synthetic earthquake slips based on random variables distributed according to a Cauchy law and a Gauss law see Figure 4 of *Lavallée and Archuleta* [2003].) These results suggest some features of the complexity recorded in tree ring indices are quite general, perhaps ''universal,'' and thus can be formulated in term of the stochastic model discussed in this letter. Five parameters are needed to completely determine the stochastic model: the four parameters of the Lévy law controlling the amplitudes of the signal fluctuations and a scaling exponent to specify the correlation.

[14] We already have indicated that the parameter α controls the rate at which the probability to observe extreme events is decreasing. That is, for dendrochronological data, large climatic departure from the ''usual'' variability observed in the data. In principle the same procedure outlined in this letter can be applied to other paleoclimatic time series such as ice core data, staglagmite data as well as to temperature time series recorded in recent years. Comparisons of the α values computed for such time series, or for different period of times, will indicate the time dependence of the parameter α, and therefore the time dependence in the rate at which the probability to observe abrupt climatic change is decreasing.

[15] **Acknowledgments.** We appreciate the thoughtful comments of the reviewers, Dr. Bodri and Dr. Putnam, who have helped to clarify the contents of this paper. We also thank Dr. Jones for his suggestions and his reading of the papers. Computations were performed using Mathematica 4.2 (Wolfram Research, Inc., 1999). The research reported in this paper was undertaken when the first author was appointed the W. F. James Professor of Pure and Applied Sciences at St. Francis Xavier University during the summer of 2003. This is ICS contribution 642.

References

Beltrami, H. (2002), Climate from borehole data: Energy fluxes and temperatures since 1500, *Geophys. Res. Lett.*, *29*(23), 2111, doi:10.1029/2002GL015702.

Beltrami, H., J. Smerdon, H. N. Pollack, and S. Huang (2002), Continental heat gain in the global climate system, *Geophys. Res. Lett.*, *29*(8), 1167, doi:10.1029/2001GL014310.

Cook, E. R., and K. R. Briffa (1990), A comparison of some tree-ring standardization methods, in *Methods of Dendrochronology: Applications in the Environmental Sciences*, edited by E. R. Cook and L. A. Kairiukstis, pp. 153–162, Kluwer Acad., Norwell, Mass.

Cook, E. R., B. M. Buckley, R. D. D'Arrigo, and M. J. Peterson (2000), Warm-season temperatures since 1600 B.C. reconstructed from Tasmanian tree rings and their relationship to large-scale sea surface temperature anomalies, *Clim. Dyn.*, *16*(2/3), 79–91.

Esper, J., K. Treydte, H. Gärtner, and B. Neuwirth (2001), A tree ring reconstruction of climatic extreme years since 1427 AD for western central Asia, *Palaeobotanist*, *50*, 141–152.

Esper, J., E. R. Cook, and F. H. Schweingruber (2002), Low-frequency signals in long tree-ring chronologies for reconstructing past temperature variability, *Science*, *295*, 2250–2253.

Falconer, K. (1990), *Fractal Geometry*, 288 pp., John Wiley, Hoboken, N. J.

Grigoriu, M. (1995), *Applied Non-Gaussian Processes*, 442 pp., Prentice Hall, Old Tappan, N. J.

Houghton, J. T., , G. J. Jenkins, and J. J. Ephraums (Ed.) (2001), *Climate Change 2001: The Scientific Basis—Contribution of Working Group I to the Third Assessment Report of the Intergovernmental Panel on Climate Change*, 881 pp., Cambridge Univ. Press, New York.

Lavallée, D., and R. J. Archuleta (2003), Stochastic modeling of slip spatial complexities for the 1979 Imperial Valley, California, earthquake, *Geophys. Res. Lett.*, *30*(5), 1245, doi:10.1029/2002GL015839.

Levitus, S., J. Antonov, J. Wang, T. L. Delworth, K. Dixon, and A. Broccoli (2001), Anthropogenic warming of the Earth's climate system, *Science*, *292*, 267–270.

Mann, M. E., R. S. Bradley, and M. K. Hughes (1999), Northern Hemisphere temperatures during the past millennium: Inferences, uncertainties, and limitations, *Geophys. Res. Lett.*, *26*, 759–762.

Peitgen, H.-O., and D. Saupe (1988), *The Science of Fractal Images*, 312 pp., Springer-Verlag, New York.

Stahle, D. W., E. R. Cook, M. K. Cleaveland, M. D. Therrell, D. M. Meko, H. D. Grissino-Mayer, E. Watson, and B. H. Luckman (2000), Tree-ring data document 16th century megadrought over North America, *Eos Trans. AGU*, *81*(12), 121, 125.

Uchaikin, V. V., and V. M. Zolotarev (1999), *Chance and Stability*, 570 pp., VSP, Utrecht, Netherlands.

H. Beltrami, Environmental Earth Sciences Laboratory, St. Francis Xavier University, Antigonish, Nova Scotia B2G 2W5, Canada. (hugo@stfx.ca)

D. Lavallée, Institute for Crustal Studies, University of California, Santa Barbara, CA 93106, USA. (daniel@crustal.ucsb.edu)